

6-2001

Nanoscale Intrinsic Localized Modes in an Antiferromagnetic Lattice

Lars Q. English
Dickinson College

M. Sato

A. J. Sievers

Follow this and additional works at: https://scholar.dickinson.edu/faculty_publications



Part of the [Physics Commons](#)

Recommended Citation

English, L.Q., M. Sato, and A.J. Sievers. "Nanoscale Intrinsic Localized Modes in an Antiferromagnetic Lattice." *Journal of Applied Physics* 89, no. 11 (2001): 6707-6709. <http://aip.scitation.org/doi/abs/10.1063/1.1362639>

This article is brought to you for free and open access by Dickinson Scholar. It has been accepted for inclusion by an authorized administrator. For more information, please contact scholar@dickinson.edu.

Nanoscale intrinsic localized modes in an antiferromagnetic lattice

L. Q. English,^{a)} M. Sato, and A. J. Sievers

Laboratory of Atomic and Solid State Physics, Cornell University, Ithaca, New York 14853-2501

The weak dissipation of spin waves in magnetic materials make antiferromagnets realistic condensed matter systems for the experimental observation of intrinsic localized modes of nanoscale size. By employing a chirped high power microwave pulse, a few microseconds long, the lowest frequency antiferromagnetic uniform mode of the quasi-one-dimensional biaxial antiferromagnet $(\text{C}_2\text{H}_5\text{NH}_3)_2\text{CuCl}_4$ has been efficiently driven into an unstable dynamical region. Intrinsic localized spin waves form below the gap. Our experimental findings demonstrate that a simple optimal control scheme can be used to investigate this kind of nonlinear excitation. © 2001 American Institute of Physics. [DOI: maximum]

I. INTRODUCTION

Both nonlinearity and lattice discreteness have played important roles in many branches of condensed matter physics. As evidenced by the appearance of domain walls, kinks, and solitons, nonlinearity cannot be treated as a perturbation in many cases. A major recent advance of the theory of nonlinear excitations in discrete lattices was the discovery that some localized vibrations in perfectly periodic atomic lattices can be stabilized by lattice discreteness. This realization has led to extensive studies of the features associated with intrinsic localization in various nonlinear lattices, and it has proven to be a conceptual and practical breakthrough.¹⁻³ These localized excitations are often called “intrinsic localized modes” (ILMs) with the emphasis on the fact that their formation involves no disorder and that they extend over a nanolength scale. The earlier work of the last decade has recently been formalized in terms of a number of useful existence and stability criteria,² and many physically exciting contexts are currently emerging—in nonlinear crystal dynamics,³⁻⁵ magnetic systems,⁶⁻⁹ electron-phonon systems,¹⁰ reaction dynamics,¹¹ molecular biophysics¹² and lattice-assisted energy/charge transfer in polarizable, soft condensed and biological matter.¹³

II. MODULATIONAL INSTABILITY

In 1992 a generation technique was proposed¹⁴ valid for all lattice scales which involves the instability of a large amplitude uniform mode. It was recognized that the instability could be used for the indirect generation of nanoscale ILMs. In the context of anharmonic atomic lattices, it was found with numerical simulations¹⁵ that a chirped excitation pulse (optimal control scheme) in the optical phonon frequency region would be most suitable for generating vibrational localization; however, the required amplitudes and chirping rates exceeded the limitations of available infrared sources.

From the experimental point of view, the investigation of nanoscale localization of nonlinear spin lattice modes has definite advantages over the vibrational case because the dis-

sipation of spin waves in magnetic materials is much slower. The large amplitude uniform mode of antiferromagnetic spin systems with anisotropy was studied in some detail, and the uniform mode was predicted to break up into stable nanoscale ILM excitations within the gap when the dispersion curve had positive curvature at $k=0$.¹⁶

An appropriate system is the layered antiferromagnet $(\text{C}_2\text{H}_5\text{NH}_3)_2\text{CuCl}_4$ where the effective one-dimensional Hamiltonian is

$$H = 2J_{\text{AF}} \sum_n \vec{S}_n \cdot \vec{S}_{n+1} + \sum_n \vec{S}_n \cdot \vec{D} \cdot \vec{S}_n + \frac{1}{2} \sum_{n,n'} \vec{S}_n \cdot \vec{F}(n-n') \cdot \vec{S}_{n'}. \quad (1)$$

Here \vec{S}_n is the effective spin of the n th layer, and is treated as a classical vector. The antiferromagnetic exchange constant $J_{\text{AF}} > 0$, and the anisotropy tensor \vec{D} arise from the anisotropic ferromagnetic exchange interaction between spins belonging to the same layer. The third term describes the dipole-dipole interactions where $\vec{F}(n-n')$ is the effective dipolar interaction tensor between spins belonging to the n th and n' th layers.⁸ The result is a biaxial antiferromagnet in which the lowest frequency dispersion curve has the required positive curvature as shown in Fig. 1. Although the uniform mode is in the microwave frequency region the desired ILM mode will appear at still lower frequencies as shown in the lowest frame.

Figure 2 shows the breakup of a large amplitude uniform mode as a function of time for a dispersion curve with positive curvature as determined from molecular dynamics (MD) simulations. The wave-vector (p) evolution is shown in Fig. 2(a) while the real space (n) dynamics are presented in Fig. 2(b).¹⁶

III. EXPERIMENTAL DETAILS

The $(\text{C}_2\text{H}_5\text{NH}_3)_2\text{CuCl}_4$ single crystals are grown from an aqueous solution of ethylamine hydrochloride and copper (II) chloride by slow evaporation. These crystals have been measured at 1.2 K. The pump-probe experiment incorporates two independent microwave sources, as shown in Fig. 3. The

^{a)}Electronic mail: quentin@ccmr.cornell.edu

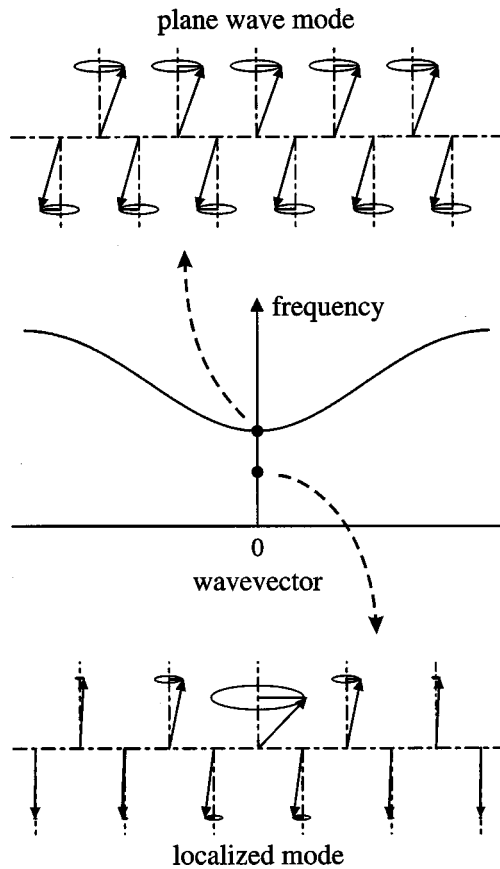


FIG. 1. *Top*—The uniform mode spin wave and dispersion curve for small amplitude excitations in antiferromagnet. *Bottom*—An ILM, which because of nonlinearity+periodicity is stable in the same lattice.

first source is a voltage controlled oscillator driven by a ramp voltage generator to produce a chirped microwave signal. Thus, the frequency position of the microwave pump can be controlled via the applied voltage ramp. Short pulses ($\sim 5 \mu\text{s}$) of this chirped pump are then created by a diode switch, and subsequently amplified to a maximum power of 40 W by a high-power solid-state amplifier.

The second source generates a weak continuous wave (cw) tunable signal and constitutes the probe beam. Pump and probe beams are combined by a coupler and delivered to the ac-field loop surrounding the sample via a circulator. After removal of the reflected pump pulse by a second switch, the reflected signal is detected by a receiver, tuned to the second oscillator, and recorded by an oscilloscope. A spectrum analyzer functioned as this receiver. The output bandwidth is set to 3 MHz for highest time resolution. Both switches, the ramp generator and the oscilloscope are synchronized by a pulse generator (not shown).

Spectra are obtained by recording the reflected power as a function of time at fixed frequency and then incrementing the frequency of the probe oscillator. It is crucial that the signal is resolved in both frequency and time to observe the growth and decay of the broad spectral features connected with ILM production. Some turning of the antiferromagnetic resonance frequency is possible by applying a dc magnetic field along the easy (second-easy) axis which increases (decreases) the antiferromagnetic resonance (AFMR) frequency.

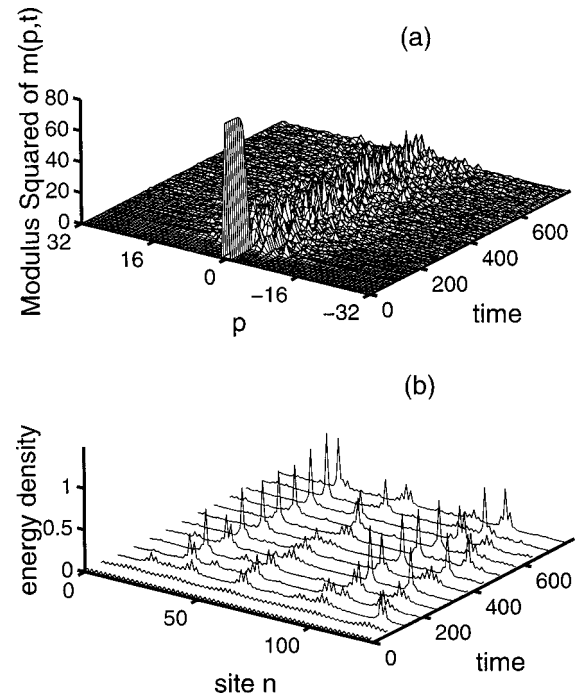


FIG. 2. According to MD simulations the large amplitude uniform spin mode is unstable as a function of time (top frame) because of the nonlinearity of the magnetic coupling and the positive curvature of the dispersion curve. The development of ILMs is most easily seen in the real space representation (bottom frame). (After Ref. 16.)

IV. EXPERIMENTAL RESULTS

Pump-probe measurements were done at various power levels, pulse widths, and chirp rates. Figure 4 shows typical time dependent data where the parameters of the pump pulse were chosen to most clearly exhibit the breakup of the AFMR into ILMs. The linear AFMR spectrum is the dotted curve at the bottom of Fig. 4. As indicated by the spectrum at the top of the figure, the AFMR vanishes after the application of the pump pulse. What replaces it is a very broad, flat spectrum attributed to the emergence of ILMs with varying

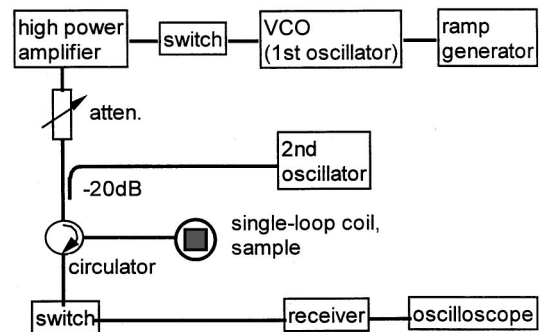


FIG. 3. Schematic experimental setup for the measurement. An intense chirped microwave pump pulse is produced by a high power amplifier driven by a voltage-controlled oscillator. A low power cw microwave probe from a tunable second oscillator is coupled to the single-loop coil through a circulator. The reflected probe signal is detected by a spectrum analyzer, used as a receiver tuned to the second oscillator, and recorded by an oscilloscope. The switch before the spectrum analyzer eliminates the pump. All switches, the ramp generator, and the oscilloscope are synchronized by a pulse generator (not shown).

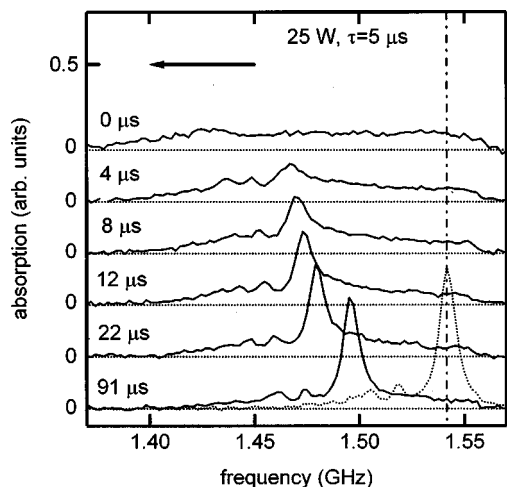


FIG. 4. Time development of the absorption spectrum after the excitation pulse. The time sequence after the end of the $5 \mu\text{s}$ pulse is identified in the figure. The dotted spectrum is a low power trace before the pulse. The pulse chirping from 1.45 to 1.40 GHz is indicated by the arrow. Peak pulse power: 25 W; width: $5 \mu\text{s}$.

degrees of localization. In the subsequent time cuts, a gradual reappearance and buildup of the uniform mode is observed at the expense of the broad features in the spectrum. The total area under the absorption curve stays constant in time (within experimental error). These data indicate that ILMs live for up to $\sim 12 \mu\text{s}$. The small AFMR peak first appears in the ILM spectrum at $\sim 5 \mu\text{s}$, indicating that some ILMs disappear even at these short times. The time evolution in Fig. 4 shows that the energy is transferred from ILMs to the uniform mode. After about $20 \mu\text{s}$ the spectrum contains only a nonlinearly excited AFMR, which then relaxes back to its small amplitude frequency with a time constant $T_1 \sim 3 \text{ ms}$.

V. CONCLUSIONS

The experimental evidence for these self-localized, but movable, excitations in nonequilibrium atomic lattices is finally evident. These efforts devoted to examining the nonlinear dynamics of lattices with nanoscale spacing have gen-

erated other possible applications for ILMs such as in friction,¹⁷ and crack propagation.¹⁸ Developing areas involving large-scale lattices which deal with ILMs in Josephson arrays,^{19,20} localized E and M modes in optical switches²¹ and in nonlinear photonic crystal wave guides.^{22,23} The next experimental challenge will be to identify nonlinear localized excitations in discrete quantum lattices.

ACKNOWLEDGMENTS

The authors thank H. Padamsee for providing much of the microwave equipment used in these experiments. This work is supported by NSF-DMR 9979483.

- ¹A. J. Sievers and J. B. Page, in *Dynamical Properties of Solids: Phonon Physics The Cutting Edge*, Vol. VII, edited by G. K. Norton and A. A. Maradudin (North Holland, Amsterdam, 1995), pp. 137–255.
- ²S. Aubry, *Physica D* **103**, 201 (1997).
- ³S. Flach and C. R. Willis, *Phys. Rep.* **295**, 181 (1998).
- ⁴S. R. Bickham, S. A. Kiselev, and A. J. Sievers, in *Spectroscopy and Dynamics of Collective Excitations in Solids*, Vol. 356, edited by B. D. Bartolo (Plenum, New York, 1997), p. 247.
- ⁵K. O. Rasmussen, S. Aubry, A. R. Bishop, and G. P. Tsironis, *Eur. Phys. J. B* **15**, 169 (2000).
- ⁶R. F. Wallis, D. L. Mills, and A. D. Boardman, *Phys. Rev. B* **52**, R3828 (1995).
- ⁷S. Rakhmanova and D. L. Mills, *Phys. Rev. B* **58**, 11 458 (1998).
- ⁸R. Lai and A. J. Sievers, *Phys. Rep.* **314**, 147 (1999).
- ⁹U. T. Schwarz, L. Q. English, and A. J. Sievers, *Phys. Rev. Lett.* **83**, 223 (1999).
- ¹⁰H. Fehske, G. Wellein, H. Buttner, A. R. Bishop, and M. I. Salkola, *Physica B* **281**, 673 (2000).
- ¹¹P. Maniatis, G. P. Tsironis, A. R. Bishop, and A. V. Zolotaryuk, *Phys. Rev. E* **60**, 7618 (1999).
- ¹²M. Peyrard, *Physica D* **119**, 184 (1998).
- ¹³N. Theodorakopoulos and M. Peyrard, *Phys. Rev. Lett.* **83**, 2293 (1999).
- ¹⁴Y. S. Kivshar and M. Peyrard, *Phys. Rev. A* **46**, 3198 (1992).
- ¹⁵T. Rössler and J. B. Page, *Phys. Rev. Lett.* **78**, 1287 (1997).
- ¹⁶R. Lai and A. J. Sievers, *Phys. Rev. B* **57**, 3433 (1998).
- ¹⁷O. M. Braun and Y. S. Kivshar, *Phys. Rev. B* **43**, 1060 (1991).
- ¹⁸J. E. Hammerberg, B. L. Holian, J. Roder, A. R. Bishop, and S. J. Zhou, *Physica D* **123**, 330 (1998).
- ¹⁹E. Trias, J. J. Mazo, and T. P. Orlando, *Phys. Rev. Lett.* **84**, 741 (2000).
- ²⁰P. Binder, D. Abraimov, A. V. Ustinov, S. Flach, and Y. Zolotaryuk, *Phys. Rev. Lett.* **84**, 745 (2000).
- ²¹O. Bang and P. D. Miller, *Opt. Lett.* **21**, 1105 (1996).
- ²²A. R. McGurn, *Phys. Lett. A* **251**, 322–335 (1999).
- ²³A. R. McGurn, *Phys. Rev. B* **61**, 13 235 (2000).